Instantaneous complex conjugate resolved spectral domain and swept-source OCT using 3x3 fiber couplers

Marinko V. Sarunic, Michael A. Choma, Changhuei Yang, Joseph A. Izatt

Department of Biomedical Engineering, Duke University, Durham, NC 27708
jizatt@duke.edu

Abstract: We report that the complex conjugate artifact in Fourier domain optical coherence tomography approaches (including spectral domain and swept source OCT) may be resolved by the use of novel interferometer designs based on 3x3 and higher order fiber couplers. Interferometers built from NxN (N>2) truly fused fiber couplers provide simultaneous access to non-complementary phase components of the complex interferometric signal. These phase components may be converted to quadrature components by trigonometric manipulation, then inverse Fourier transformed to obtain A-scans and images with resolved complex conjugate artifact. We demonstrate instantaneous complex conjugate resolved Fourier domain OCT using 3x3 couplers in both spectral domain and swept source implementations. Complex conjugate artifact suppression by factors of ~20dB and ~25dB are demonstrated for spectral domain and swept source implementations, respectively.

OCIS code: (110.4500) Optical coherence tomography

References and links

1. D. Huang, E. A. Swanson, C. P. Lin, J. S. Schuman, W. G. Stinson, W. Chang, M. R. Hee, T. Flotte, K. Gregory,C. A. Puliafito, "Optical coherence tomography," Science **254**, 1178-1181 (1991).
2. A. F. Fercher, C. K. Hitzenberger, G. Kamp, and S. Y. Elzaiat, "Measurement of Intraocular Distances by Backscattering Spectral Interferometry," Opt. Commun. **117**, 43-48 (1995).
3. S. R. Chinn, E. A. Swanson, and J. G. Fujimoto, "Optical coherence tomography using a frequency-tunable optical source," Opt. Lett. **22**, 340-342 (1997).
4. R. A. Leitgeb, C. K. Hitzenberger, and A. F. Fercher, "Performance of fourier domain vs. time domain optical coherence tomography," Opt. Express **11**, 889-894 (2003), http://www.opticsexpress.org/abstract.cfm?URI=OPEX-11-8-889
5. M. A. Choma, M. V. Sarunic, C. Yang, and J. A. Izatt, "Sensitivity advantage of swept source and Fourier domain optical coherence tomography," Opt. Express **11**, 2183-2189 (2003), http://www.opticsexpress.org/abstract.cfm?URI=OPEX-11-18-2183
6. J. F. de Boer, B. Cense, B. H. Park, M. C. Pierce, G. J. Tearney, and B. E. Bouma, "Improved signal-to-noise ratio in spectral-domain compared with time-domain optical coherence tomography," Opt. Lett. **28** 2067-2069 (2003).
7. R. A. Leitgeb, C. K. Hitzenberger, and A. F. Fercher T. Bajraszewski "Phase-shifting algorithm to achieve high-speed long-depth-range probing by frequency-domain optical coherence tomography," Opt. Lett. **28** 2201-2203 (2003)
8. M. Wojtkowski, A. Kowalczyk, R. Leitgeb, and A. F. Fercher "Full range complex spectral optical coherence tomography technique in eye imaging," Opt. Lett. **27**, 1415-1417 (2002).
9. S. H. Yun, G. J. Tearney, J. F. de Boer, and B. E. Bouma, "Removing the depth-degeneracy in optical frequency domain imaging with frequency shifting," Opt. Express **12,** 4822-4828 (2004), http://www.opticsexpress.org/abstract.cfm?URI=OPEX-12-20-4822
10. M. A. Choma, C. Yang, and J.A. Izatt, "Instantaneous Quadrature Low Coherence Interferometry With 3x3 Fiber Optic Couplers," Opt. Lett. **28** , 2162-2164 (2003)

#5957 - $15.00 US Received 2 December 2004; revised 28 January 2005; accepted 30 January 2005

11. N. A. Nassif, B. Cense, B. H. Park, M. C. Pierce, S. H. Yun, B. E. Bouma, G. J. Tearney, T. C. Chen, and J. F. de Boer, "*In vivo* high-resolution video-rate spectral-domain optical coherence tomography of the human retina and optic nerve," Opt. Express **12,** 367-376 (2004), http://www.opticsexpress.org/abstract.cfm?URI=OPEX-12-3-367
12. A. W. Snyder, "Coupled-Mode Theory for Optical Fibers," J. Opt. Soc. Am. **62**, 1267-1277 (1972).
13. M.A. Choma, M.V. Sarunic, C. Yang, K.Hsu, J.A. Izatt, "Sensitivity Advantage of Swept Source and Fourier Domain Optical Coherence Tomography," presented at *Coherence Domain Optical Methods and Optical Coherence Tomography in Biomedicine VIII*, SPIE, San Jose, January 26-28 (2004).
14. S. H. Yun, G. J. Tearney, J. F. de Boer, and B. E. Bouma, "Motion artifacts in optical coherence tomography with frequency-domain ranging," Opt. Express **12,** 2977-2998 (2004), http://www.opticsexpress.org/abstract.cfm?URI=OPEX-12-13-2977
15. S. Radhakrishnahan, A. M. Rollins, J.E. Roth, S. Yazdanfar, V. Westphal, D. S. Bardenstein, J. A. Izatt, "Real-time optical coherence tomography of the anterior segment at 1310 nm," Archives of Ophthalmology, 119, 1179-85 (2001).
16. N. A. Nassif, B. Cense, B. H. Park, M. C. Pierce, S. H. Yun, B. E. Bouma, G. J. Tearney, T. C. Chen, and J. F. de Boer, "In vivo high-resolution video-rate spectral-domain optical coherence tomography of the human retina and optic nerve," Opt. Express **12**, 367-376 (2004), http://www.opticsexpress.org/abstract.cfm?URI=OPEX-12-3-367
17. S. H. Yun, G. J. Tearney, J. F. de Boer, N. Iftimia, and B. E. Bouma, "High-speed optical frequency-domain imaging," Opt. Express **11**, 2953-2963 (2003), http://www.opticsexpress.org/abstract.cfm?URI=OPEX-11-22-2953

1. Introduction

Fourier domain techniques in optical coherence tomography (OCT) [1,2,3] have received much attention in recent literature due to the significant sensitivity advantage over time domain OCT [4,5,6]. In Fourier domain OCT (FDOCT), the positions of scatterers in a sample are resolved by acquiring the optical spectrum of sample light interfered with light from a single stationary reference reflector using a Michelson type interferometer. There are two primary implementations of FDOCT, dependent on the type of light source and detector combination used. Spectral domain OCT (SDOCT) utilizes the low coherence source standard in time domain OCT systems, but in the detector arm disperses the interferometric signal spectrum across an array detector using a spectrometer [2]. (These definitions of FDOCT and SDOCT have been reversed by some previous authors [e.g., 4], but appear to be the current consensus). In swept source OCT (SSOCT), also referred to in the literature as optical frequency-domain imaging (OFDI), the spectrum is acquired in a single detector by temporally sweeping the source spectrum [3].

An NxN FDOCT system may be constructed by adapting the standard Michelson type interferometer with a higher order fused fiber coupler. Simple 3x3 FDOCT and SSOCT system topologies constructed this way are illustrated in Fig. 1. In both SSOCT and SDOCT, the current measured in the mth spectral channel of the i^{th} detector or spectrometer, denoted by $\hat{D}_i[k_m]$, is proportional to:

$$\hat{D}_i[k_m] \propto \rho \cdot \hat{S}[k_m] \cdot \left(R_R + R_S + 2\sqrt{R_R R_S}\cos(2\Delta x k_m + \varphi_i)\right), \quad (1)$$

where $\hat{S}[k_m]$ is the source spectral density in units of watts per wavenumber, R_S and R_R represent the reflectivity of the object in sample and reference arm, respectively, and φ_i is the phase shift of the interferometric signal associated with the i^{th} detector signal. The detector responsivities, assumed to be uniform, are denoted by ρ, and the detector elements are indexed by $m \in \{1,M\}$, where M is the number of detector pixels in SDOCT or the number of spectral samples in SSOCT. The round-trip displacement of each sample reflection from the reference

#5957 - $15.00 US Received 2 December 2004; revised 28 January 2005; accepted 30 January 2005

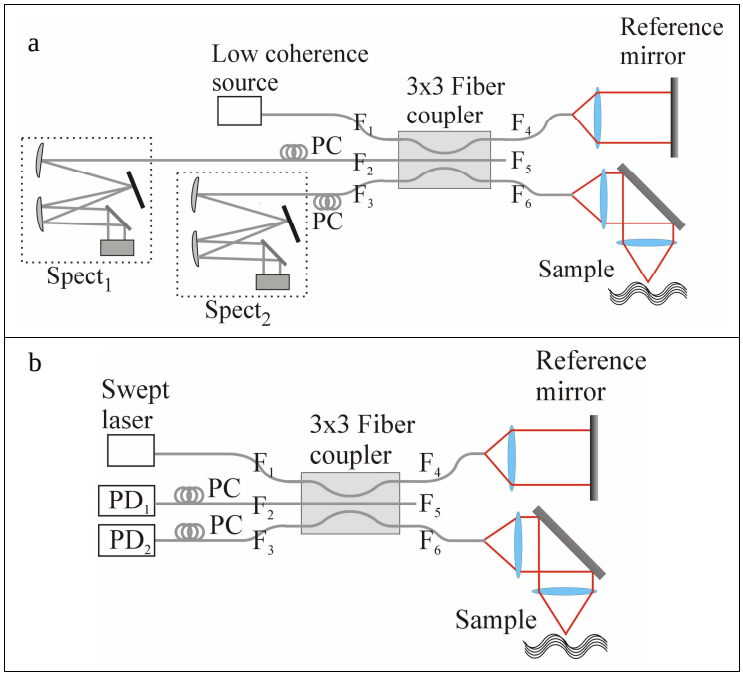

Fig. 1. Fourier domain OCT systems employing 3x3 truly fused fiber couplers. (a) For SDOCT systems, a broadband source is used to illuminate the sample. Multiple spectrometers, $Spect_n$, with detector arrays may be used in the detector arms. (b) For SSOCT systems, the source is narrowband and swept in frequency, and the detectors PD_n represent single-channel photoreceivers. F_n are input and output fibers of the couplers. PC, polarization controller; ADC, analog to digital converter; CPU, computer.

path length is encoded by the frequency of cosinusoidal variations of $\hat{D}_i[k_m]$, while the sample reflectivity is encoded in the visibility of these variations. The spectrally indexed detector outputs therefore represent the real part of the discrete Fourier transform of an OCT A-scan, given by [5]:

$$D_i[x_n] = \sum_{m=1}^{M} \hat{D}_i[k_m] e^{-\left(j2\pi(2k_m x_n)\right)}, \quad n \in \left\{1, M\right\} \tag{2}$$

The factor of 2 in the kernel exponent ensures the recovery of single-sided distances, and M is the number of spectral samples. In the x-domain, the channel spacing is $\delta x = 1/\Delta k$, where Δk is the bandwidth of the source in wavenumber units, and the scan depth is ideally $\Delta x_{max} = 1/\delta k$, where δk is the wavenumber spacing between spectral samples. However, because the A-scan is Hermitian symmetric (as will be discussed below) the effective scan depth in the absence of complex conjugate artifact resolution is $\Delta x_{max} = 1/(2\delta k)$.

Qualitatively, Eq. (2) has three peaks for the case of a single reflector in the sample arm with path length difference from the reference path of Δx. The origin of the three peaks is made clear from the Fourier transform of Eq. (1):

$$D_i[x_n] \propto S[x_n] \otimes \left[(R_R + R_S)\delta(x_n) + 2\sqrt{R_R R_S}\left(\delta(x_n + \Delta x) + \delta(x_n - \Delta x)\right)\right]. \tag{3}$$

A central peak located at x=0, referred to as the DC artifact, arises from the convolution of the Fourier transform of the source spectrum, $\hat{S}[k_m]$, with non-interfering reflected light components (the first term inside the brackets in Eq. (3)). Two additional peaks are located at

#5957 - $15.00 US Received 2 December 2004; revised 28 January 2005; accepted 30 January 2005

$x_n = \pm\Delta x$, placed symmetrically around the DC artifact, and are due to the convolution of $S[x_n]$ with the peaks at $\pm\Delta x$ from the transform of the cosine term. In consequence, a reflection at $+\Delta x$ cannot be distinguished from a reflector at $-\Delta x$; this ambiguity is referred to as the complex conjugate artifact and cannot be removed by post-processing [7,8,9].

2. Theory of complex conjugate artifact resolution

The complex conjugate artifact arises because the interferometric signal acquired in FDOCT only represents the real component of a complex waveform. The complex part of the signal must also be acquired in order to resolve this artifact. The imaginary component of the signal can be indirectly obtained by acquiring a second interferogram shifted in phase by $\pi/2$. Combining the real and imaginary parts yields the complex interferometric signal [10]:

$$\hat{D}_i[k_m] = \hat{D}_i^0[k_m] + j\hat{D}_i^{90}[k_m]. \tag{4}$$

Taking the Fourier transform of the complex interferometric signal given by Eq. (4) generates an A-scan with the position of the sample arm reflector unambiguously determined:

$$\hat{D}_i[k_m] \propto \hat{S}[k_m] \cdot \left(2(R_R + R_S) + 2\sqrt{R_R R_S}\cos(2\Delta x k_m + \varphi_i) + j2\sqrt{R_R R_S}\sin(2\Delta x k_m + \varphi_i)\right), \tag{5a}$$

$$D_i[x_n] \propto S[x_n] \otimes \left[2(R_R + R_S)\cdot\delta(x_n) + 4\sqrt{R_R R_S}\,\delta(x_n + \Delta x)\right]. \tag{5b}$$

In order to remove the DC artifact, a third spectrum representing the spectral shape of the source must also be acquired. Since the reference arm power is commonly much higher than the amount of light returned from the sample arm, a representative DC spectrum can be acquired by blocking the sample arm and collecting light returned from the reference arm only. Alternatively, when many A-scans from different sample regions are available, as when acquiring a B-scan, a representative DC spectrum can be obtained by averaging over all of the collected spectra, under the assumption that the interferometric components of the A-scans will tend to cancel out [11]. With the DC spectrum acquired by either technique, the complex signal with the DC component removed is given by:

$$\hat{D}_i[k_m] = \left(\hat{D}_i^0[k_m] - \hat{D}_i^{DC}[k_m]\right) + j\left(\hat{D}_i^{90}[k_m] - \hat{D}_i^{DC}[k_m]\right), \tag{6}$$

where the $\hat{D}_i^{DC}[k_m]$ term represents the source spectrum indexed by wavenumber.

In previous implementations of complex SDOCT, phase shifting interferometry techniques have been exploited to dither the phase of the reference electric field using a PZT mounted mirror in the reference arm. A method to obtain the complex signal using only two phase stepped scans has been proposed [7], but high quality tissue imaging has only been demonstrated using a 5 step algorithm [8] in which the additional phase steps were necessary to compensate for phase errors. An additional limitation of the phase stepping method is that since the phase stepped spectra are necessarily acquired sequentially, the reconstructed image quality is sensitive to sub-wavelength interferometric drift between phase-shifted acquisitions. To the best of our knowledge, phase shifting to resolve the complex conjugate ambiguity has not yet been reported in SSOCT, although the advantages and disadvantages of this approach should be similar as for SDOCT. A heterodyne method has been reported for SSOCT using acousto-optic modulators (AOM) to shift the interferometric signal frequency spectrum away from zero frequency, allowing positive and negative displacements to be distinguished [9].

#5957 - $15.00 US Received 2 December 2004; revised 28 January 2005; accepted 30 January 2005

An alternative solution for complex signal acquisition in FDOCT consists of making use of the intrinsic, non-complementary phase relationships which exist between light returning from interferometers constructed from higher order (NxN) fiber couplers [12]. For example, a Michelson-type interferometer constructed using a truly fused 3x3 coupler having an even power splitting ratio between the ports ideally exhibits a phase delay between detector ports of 120^o [10]. Other phase delays (including 90^o) may be obtained by use of 3x3 couplers with non-even splitting ratios, or by use of couplers with higher port counts [10]. A FDOCT system capable of simultaneously acquiring two phase shifted interferograms by using a 3x3 coupler in a Michelson type interferometer is illustrated in Fig. 1. The interferometric signals acquired at detectors D_1 and D_2 in Fig. 1 may be converted to quadrature components (0^o and 90^o) using a simple trigonometric relationship, assuming the exact splitting ratios of the coupler are known. Defining either one of the acquired spectra as the real part of the complex signal, $i_n=i_{Re}$, the imaginary part i_{Im} is obtained from the signals i_n and i_m using the cosine sum rule [10]:

$$i_{Im} = \frac{i_n \cos(\Delta\phi_{mn}) - \beta_{mn}\, i_m}{\sin(\Delta\phi_{mn})}\,. \tag{7}$$

Here, $\Delta\phi_{mn} = \phi_m - \phi_n$ is the phase difference, and β_{mn} the wavelength dependent power splitting ratio, between detector ports D_m and D_n of the interferometer. Both $\Delta\phi_{mn}$ and β_{mn} are functions of the coupling coefficients α_{ab} which characterize the wavelength dependent transfer of power from fiber F_a to fiber F_b (referring to Fig. 1) [10].,

3. Methods

3.1. SDOCT implementation

An instantaneous complex SDOCT system was constructed using the interferometer topology illustrated in Fig. 1. The source was a superluminescent diode (Superlum) with center wavelength λ_o=842nm and FWHM of $\Delta\lambda$=47nm, and the truly fused 3x3 fiber coupler was obtained from AC Photonics, Inc. Each detector arm contained a semi-custom commercially available Czerny Turner spectrometer (Thero-Oriel 157i, input focal length 127cm, numerical aperture NA = 0.13) with 1200 l/mm reflective grating blazed at 750nm. The detectors used were matched 1024 element infrared enhanced photodiode arrays (Hamamatsu, 2.5mm tall elements, 25μm pitch, 500Hz line rate). The spectrometer configuration had a spectral range of 110nm. A –3dB roll off in sensitivity was measured at a sample distance of 400μm from DC, corresponding to a spectral resolution of 0.4nm which is consistent with the supplier specifications [4]. Insertion losses of -16dB were measured in each of the spectrometers, due to grating losses, detector responsivity ($\rho \approx 0.3$), and imperfect matching of the fiber numerical aperture (specified NA of 0.10 – 0.14) to that of the spectrometer. Careful calibration of the spectrometers was required, as were phase locked control electronics to coordinate simultaneous signal collection from the two array detectors.

The spectrometers were used to measure the 9 coupling coefficients, α_{ab}, which characterized the transfer of power from fiber F_a to fiber F_b in the 3x3 coupler. The results, shown in Fig. 2(a), demonstrate that the splitting ratios of the fiber coupler were strongly

#5957 - $15.00 US Received 2 December 2004; revised 28 January 2005; accepted 30 January 2005

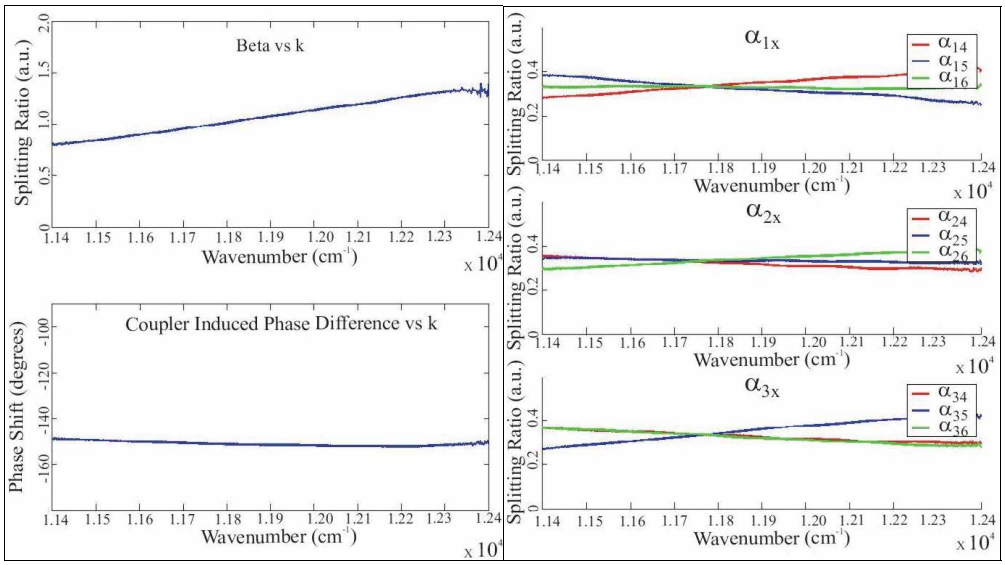

Fig. 2. (a) Coupling coefficients measured as a function of wavenumber for the 3x3 coupler. (b) The derived curves for β and $\Delta\phi$ from the coupling coefficients.

wavelength dependent. The measured coupling coefficients were used to calculate the values of $\Delta\phi_{mn}$ and β_{mn}, shown in Fig. 2(b), as described by Choma [10].

Following acquisition of simultaneous multiple phase spectral data from samples of interest, Eq. (7) was used to convert the measured spectra into quadrature components using the calibrated values of $\Delta\phi_{mn}$ and β_{mn}. The derived signals i_{Re} and i_{Im} were then re-sampled from linearly spaced samples in wavelength to be linearly spaced in wavenumber using a cubic spline interpolation [10]. This operation is required because the Fourier transform relates k-space to distance, and the FFT algorithm assumes evenly spaced samples. The complex conjugate resolved A-scans were then obtained by inverse Fourier transform of the re-sampled complex signal.

3.2. SSOCT implementation

A 3x3 SSOCT system was constructed using a swept laser designed in collaboration with Micron Optics, Inc. [13]. The swept source had a central wavelength of 1318nm, a FWHM bandwidth of 89nm, and sweep rate of 250 Hz. Because the swept source operated in the 1300nm wavelength range, commercial fiber circulators were available to recover the signal light returned to the source arm. Improving on the system used in the 3x3 SDOCT system, Fig. 3 illustrates a 3x3 SSOCT system employing a novel topology in which the signal light in the source arm was used to dynamically remove the DC component of the interferometric signal by use of balanced photodetectors (NewFocus). An AC Photonics truly fused 3x3 coupler was used to construct the Michelson type interferometer for the complex SSOCT system. The signal was digitized using an external trigger obtained by passing a portion of the laser output through a Fiber Fabry Perot (FFP) cavity [13]. This "k-trigger" provided a pixel clock signal for the analog to digital converter which was evenly spaced in wavenumber, allowing the interferometric spectra to be sampled linearly in wavenumber, thus no re-sampling of the data was required in software. The swept laser was driven with a triangular waveform, at 250Hz, but data was collected only during a single sweep direction making the effective A-scan integration time 2ms. With 1.3mW available at the sample arm, the theoretical maximum SNR was 127dB. The signal was digitized using a 14-bit analog to digital converter clocked by the k-trigger, with simultaneous sampling on the two signal channels.

#5957 - $15.00 US Received 2 December 2004; revised 28 January 2005; accepted 30 January 2005

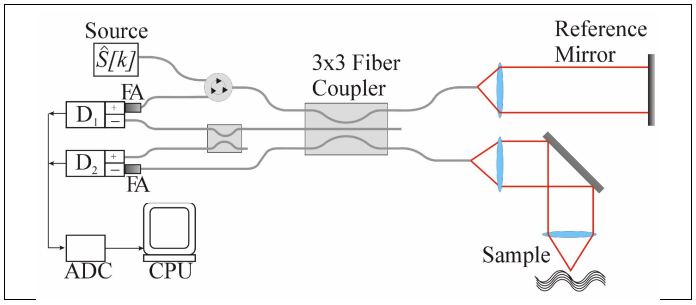

Fig. 3. 3x3 Swept source (SSOCT) system topology using a swept-wavenumber laser. A circulator recovers the signal light in the source arm, and DC signal subtraction is accomplished using balanced photodiode detectors D_1 and D_2. FA, fiber attenuators.

4. Results

4.1. 3x3 SDOCT A-scans

The performance of complex conjugate ambiguity resolution in FDOCT can be quantified by comparing complex conjugate resolved A-scans with unresolved A-scans. For this comparison, measurements were taken using the 3x3 SDOCT system illustrated in Fig.1 with a –50dB reflector in the sample arm. The DC component was subtracted by measuring the reference arm spectrum with the sample arm blocked. The interferometric portion of the signal acquired at both photodiode arrays for a single reflector in the sample arm is illustrated in Fig. 4(a), and the corresponding A-scan from a single detector output is illustrated in Fig. 4(b). The quadrature signal was obtained using the values of $\Delta\phi_{mn}$ and β_{mn} derived from measurements

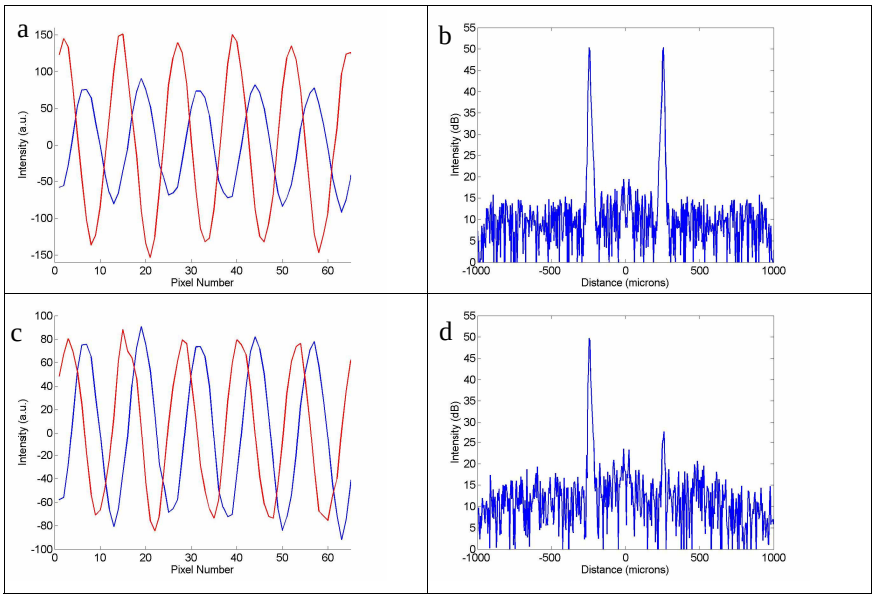

Fig. 4. Resolving the complex conjugate artifact using a 3x3 SDOCT system. (a) The interferometric signals measured on spectrometers 1 and 2 in Fig. 1 were separated by ~150°. (b) A-scan obtained by inverse Fourier transform of a single spectrum includes the complex conjugate artifact (DC component has been subtracted out). (c) The processed real (0°) and complex (90°) components of the spectra derived from Eq. (7) maintain a 90° phase difference. (d) A-scan obtained by inverse Fourier transform of the complex signal suppresses the complex conjugate peak by >20dB, revealing the reflector position to the left of DC with small artifacts on the right side and at zero displacement.

#5957 - $15.00 US Received 2 December 2004; revised 28 January 2005; accepted 30 January 2005

of the 3x3 coupler coupling coefficients (Fig. 2) together with Eq. (7), and is plotted in Fig. 4(c). The complex conjugate resolved A-scan, obtained by taking the inverse Fourier transform of the complex signal, is shown in Fig. 4(d). The data indicates a suppression of the complex conjugate peak by >20dB. The remaining artifacts at DC and a ghost remnant of the negative image of the reflector observed in the resolved A-scan were likely due to mismatches in the spectrometer alignments. The height of the suppressed complex conjugate artifact peak was measured to be relatively constant as a function of depth, as shown in Fig. 5(a). The peak SNR of the complex conjugate resolved SDOCT system was measured as ~98dB with 1mW of power in the sample arm and an integration time of 2ms. Including 16dB of measured losses in the spectrometers, the net attainable SNR was 114dB, in reasonable agreement with the predicted attainable maximum SNR of 121dB.

4.2. 3x3 SSOCT A-scans

Results from the SSOCT setup were obtained using a similar procedure to that described for the SDOCT system above, with the exception that DC subtraction in the SSOCT setup was accomplished using the balanced detection approach illustrated in Fig. 3. Although the swept laser had a narrow line width of ~0.116nm, the imaging depth was limited to ~4mm by the sampling resolution. For a sample arm power of 1.3mW and an integration time of 2ms, the 3x3 SSOCT system had a maximum SNR of 112dB near DC, which fell off to 100dB at 4mm. The observed attenuation of the complex conjugate peak had a maximum value of ~25dB near DC, and decreased to 18dB at 4mm. These details are evident in the SSOCT system performance graph in Fig. 5(b). Also seen is an artifact remaining at zero position ~30dB above the noise floor after DC subtraction using only the balanced photo-detectors. Reflections from the second surface of the neutral density filter used to attenuate the light in the sample arm of the interferometer appear as echoes to the right of the main peak in Fig. 5(b).

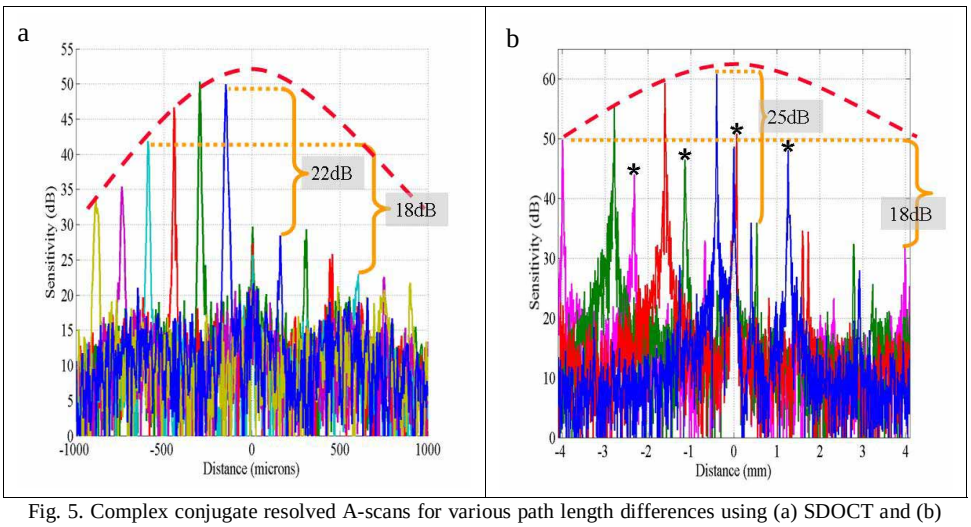

Fig. 5. Complex conjugate resolved A-scans for various path length differences using (a) SDOCT and (b) SSOCT setups taken with a –50dB reflector in the sample arm. In the SDOCT system (a), the peak SNR was ~98dB, with a peak complex conjugate artifact suppression of >20dB. For the SSOCT system (b), the peak SNR was 112dB, with a maximum suppression of the complex conjugate artifact of ~25dB. The echo artifacts in (b), denoted by asterisks, were due to reflections from the second surface of the attenuating filter in the sample arm.

4.3. Images

The true test of the complex signal 3x3 FDOCT systems described above is the quality of the images that they can acquire. The range of samples that can be imaged with the SDOCT

#5957 - $15.00 US Received 2 December 2004; revised 28 January 2005; accepted 30 January 2005

system was limited by the short sample depth due to the poor wavelength resolution of the spectrometers. Only fixed samples were imaged because motion to within a fraction of a wavelength during the 2ms integration time could severely decrease the system sensitivity [14]. B-scans of a plastic sheet acquired with the SDOCT system are shown in Fig. 6. The image in Fig. 6(a) was processed using only one of the detector outputs, and hence suffers from severe distortion due to complex conjugate artifact. The processed image in Fig. 6(b) used the interferometric signal from both photodiode arrays and Eq. (7) to obtain the full complex signal. The DC spectrum was obtained by computing the average of all the collected spectra in the B-scan [11]; this was performed separately for each detector. The computed DC spectrum was then subtracted from each unprocessed interferogram. An artifact at DC persisted due to imperfect subtraction of the DC signal component. Comparison of the unprocessed image with the complex conjugate resolved image clearly demonstrates that the complex conjugate artifact has been suppressed and that the usable sample depth has been doubled.

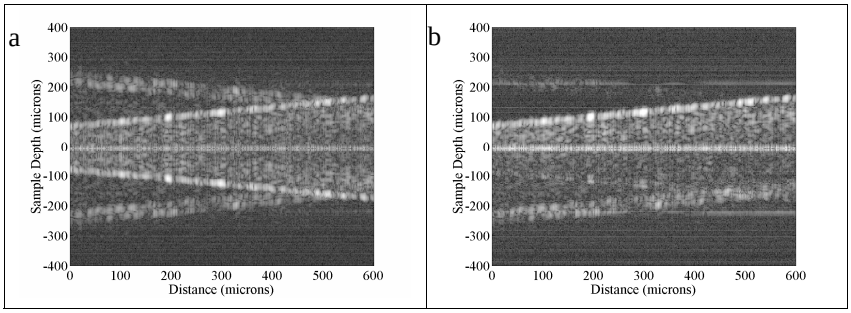

Fig. 6. B-scans of a plastic sheet using a 3x3 SDOCT system. In (a) only a single detector output was used to generate the A-scan, and the complex conjugate artifact is manifested as overlapping mirror images. (b) The full quadrature signal generated using Eq. (7) and the spectra acquired from both detectors resolves the complex conjugate ambiguity, resulting in a clear image of the sample.

The 3x3 SSOCT system was designed for use in ophthalmic anterior segment imaging, and thus required high SNR over a long sampling depth. The SSOCT system had a SNR roll-off of 12dB over 4mm (see Fig. 5(b)), but by resolving the complex conjugate artifact the imaging depth was doubled to 8mm. The extended depth range is required to image the entire anterior segment region [15]. Figure 7 contains images obtained in the anterior segment of a human eye *in vivo*. Figure 7(a) is the unprocessed image acquired using only a single detector, and is distorted by the complex conjugate artifact. In Fig. 7(b), the signals at both detectors were used with Eq. (7) (modified to account for the subtraction at the balanced photodetectors) to obtain the full complex interferometric signal and double the sampling depth by suppressing the complex conjugate artifact. In the images, additional subtraction of the DC artifact was accomplished by calculating a representative DC spectrum as the average of all the A-scans in a single image [11]. Reflective interfaces of unknown origin within the anterior segment scanning system gave rise to spurious reflective artifacts visible in the images at depths of 1.7, 2.3, and 2.6 mm.

5. Discussion

Fourier domain techniques in OCT have demonstrated a sensitivity advantage over time domain OCT. The increased sensitivity has been exploited to increase system line rates; SDOCT systems have been reported with 29kHz line rates [16], and a SSOCT system has been reported with a line rate 15.7kHz [17]. In FDOCT systems the useable sample depth is limited by the spectral resolution of the system. For SDOCT systems, the spectral resolution is

#5957 - $15.00 US Received 2 December 2004; revised 28 January 2005; accepted 30 January 2005

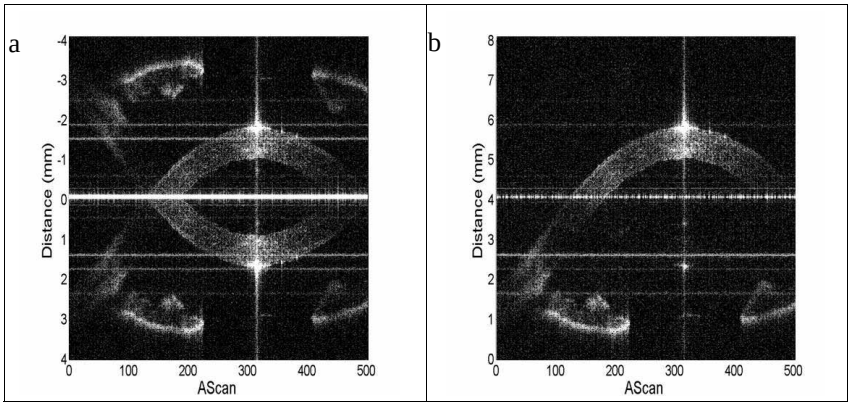

Fig. 7. B-scans taken with the 3x3 SSOCT system. In (a) only a single detector output was used to generate the A-scan, and the complex conjugate artifact is seen in overlapping mirror images. (b) The full quadrature signal generated from the acquired spectra using Eq. (7) resolved the complex conjugate ambiguity, resulting in a clear image of the sample. Unknown reflective artifacts in the scanning apparatus gave rise to spurious reflections between 1.5-2.6 mm depth, which were ambiguity resolved in (b).

decided by the spectrometers used, while for SSOCT systems the limit is ultimately set by the linewidth of the laser.

Previous phase stepping approaches for complex conjugate resolution in SDOCT required sequential scans, making the images sensitive to any interferometric drift or sample jitter between scans [7,8]. In contrast, using the outputs of a Michelson-type interferometer constructed using a 3x3 coupler, as presented in Fig. 1, simultaneously provided phase shifted interferograms at the detector ports. The interferometric signals acquired simultaneously have been processed to yield the quadrature components of the full complex interferometric signal required to obtain complex conjugate ambiguity resolved A-scans.

The SDOCT system described here had a measured SNR of 98dB, and accounting for calibrated losses in the spectrometer, fell 7dB short of the shot noise-limited theoretical SNR of 121dB. Careful alignment of the spectrometers was required to ensure that the exact same wavelength range was sampled in each corresponding pixel of the two array detectors. Slight misalignments in matching the spectrometers had strong negative effects on complex conjugate artifact suppression and appeared to be the limiting factor on system performance.

In contrast, the 3x3 SSOCT system employed simultaneous sampling on multiple ports, ensuring that identical wavenumber samples were collected at both detectors for each pulse of the k-trigger. An SNR of 112dB was measured for the 3x3 SSOCT system, falling 15dB short of the shot noise-limited theoretical SNR calculated assuming equal detector responsivities. The lower than predicted SNR can be partially attributed to attenuation of the signal at the photodetectors which was required to match signal strengths on the balanced photodiodes. The uneven wavelength dependent splitting ratios in the 3x3 coupler lead to imperfect spectrum subtraction at the balanced photodiodes, and resulted in the remaining artifact at zero displacement visible in Fig. 5(b). This appeared to be the factor limiting the resolution of complex conjugate artifact in the 3x3 SSOCT system.

The anterior segment images in Fig. 7, taken *in vivo* on a human volunteer, were post processed to further suppress the DC artifact by subtracting from each interferometric spectrum a representative DC spectrum obtained by averaging over all the A-scans in the image for each detector. Use of higher order couplers to simultaneously obtain a larger number of phase steps may improve suppression of the complex conjugate artifact to a level which has been demonstrated for *ex vivo* specimens using the PZT phase stepping method [8].

#5957 - $15.00 US Received 2 December 2004; revised 28 January 2005; accepted 30 January 2005

6. Summary

Instantaneous acquisition of the complex interferometric signal using 3x3 couplers has been demonstrated for both spectral domain OCT and swept source OCT. Processing of the phase separated spectra obtained at the output ports of the 3x3 coupler allows suppression of the complex conjugate artifact; suppression of the complex conjugate artifact of >20dB for SDOCT and >25dB for the SSOCT system was presented. By resolving the complex conjugate artifact, the maximum sample depth was doubled relative to systems using only a single detector.

Acknowledgments

This work was supported by NIH grants R21 RR019769 and R24-EB00243. The collaboration of K. Hsu and Micron Optics, Inc. is gratefully acknowledged.

#5957 - $15.00 US Received 2 December 2004; revised 28 January 2005; accepted 30 January 2005